Load-Bearing Capacity of Masonry Arch Bridges Strengthened with Fibre Reinforced Polymer Composites

J. F. Chen

School of the Built Environment, The University of Nottingham, University Park, Nottingham NG7 2RD, UK
E-mail: jianfei.chen@nottingham.ac.uk

Abstract: This paper presents a new mechanism analysis method to calculate the ultimate load-bearing capacity of masonry arch bridges strengthened by externally bonding fibre reinforced polymer (FRP) composites on the intrados. The *M–N* relationship of a strengthened arch ring cross section is analysed and fully considered in the mechanism analysis. The Complex Method of nonlinear programming is used to perform a constrained minimisation of the load function to obtain the minimum collapse load and its corresponding hinge positions. This has advantages because the arch ring does not need division into many discrete blocks as in traditional mechanism analysis and the solution process is fully automatic. Some initial results are presented, which show that significant strength increases can be achieved by bonding a small amount of FRP composites to the intrados of masonry arch bridges.

Key words: masonry arch bridge, strengthening, fibre reinforced polymer composites, FRP, mechanism analysis, the complex method

1. INTRODUCTION

Masonry arch bridges make a significant contribution to the UK's road and rail infrastructure. The majority of these were constructed in the 19th century, or even earlier (Page 1993). It is clear therefore, that they were not originally designed to carry the extent of loads imposed on them by current vehicular traffic. Many existing masonry arch bridges need reassessment of their 'fitness for purpose' and upgrading where, and as, appropriate. This situation has encouraged research in this domain in the last decade (e.g. Hughes 1995, Hughes and Blackler 1997, Hughes et al. 1998, Melbourne et al. 1997, Peaston and Choo 1996, Prentice 1996, Ponniah and Prentice 1998).

Many methods are available for strengthening masonry arch bridges. Commonly used methods include saddling, sprayed concrete and relieving arch etc. (Department of Transport 1993, Page 1993). Based on the method established by the Military Engineering Experimental Establishment (MEXE), the load bearing capacity is a direct function of the sum of the thickness of the arch barrel and the depth of fill at the crown (Peaston and Choo 1996). When the depth of fill at the crown is large, a significant amount of strengthening of

the arch barrel is often needed to meet the required increase of the load bearing capacity.

This paper reports an initial theoretical study on the strengthening of masonry arch bridges by bonding fibre-reinforced polymer (FRP) composites to the arch intrados. FRP composites are very light and provide ease of site handling, so the retrofit construction work can be performed quickly and without specialist or heavy machinery. This means minimal disturbance to traffic; an important consideration in bridge repair or rehabilitation work. Neither will the dimensions of a bridge be changed significantly, so the original appearance is maintained and, minimal loss of headroom is experienced where traffic goes under the bridge. Corrosion is not a problem in that FRP is virtually corrosion resistant. The use of FRP sheets can also prevent the development of longitudinal cracks in bridge masonry.

A new mechanism analysis method is presented in this paper, which duly considers the M–N relationship within the bridge's arch ring, to calculate the ultimate load-bearing capacity of bridges strengthened in this way. The minimal collapse load and its corresponding hinge positions are obtained by using the Complex Method to perform a constrained minimisation of the load function. This has advantages because the arch ring does not need division into many discrete blocks as in traditional mechanism analysis and the solution process is fully automatic. Some initial results are presented, which show that significant strength increases can be achieved by bonding a small amount of FRP composite to the intrados of masonry arch bridges.

2. ULTIMATE STRENGTH OF FRP STRENGTHENED RECTANGULAR CROSS-SECTION UNDER ECCENTRIC COMPRESSION

2.1. Basic Equations

The ultimate strength of an FRP strengthened rectangular masonry cross-section under eccentric compression, which closely represents the cross-section of an arch ring in a masonry arch bridge strengthened by bonding FRPs on its intrados, is analysed in this section.

A masonry cross-section of width B and thickness t is strengthened with an FRP sheet or plate with thickness t_{frp} and cross-sectional area A_{frp} (Figure 1a). This strengthened cross-section is under a bending moment M and a compressive axial force N (i.e. under a compression load N with eccentricity $e = M/N$) (Figure 1b). It is assumed here that t_{frp} is much smaller than t (i.e. $t_{frp}/t \ll 1$) and there is a perfect bond between the masonry and the FRP composite. By adopting the assumption that plane sections remain plane after deformation, the strain distribution on the cross-section can be found as shown in Figure 1c. The relationship between the strain in the FRP composite, ε_{frp}, and the strain in the masonry at the compression face, ε_m, is thus

$$\varepsilon_{frp} = \left(\frac{t}{x} - 1\right)\varepsilon_m \tag{1}$$

where x is the height of the compressive area of the masonry (Figure 1c). Subscript m denotes masonry and frp denotes FRP throughout this paper.

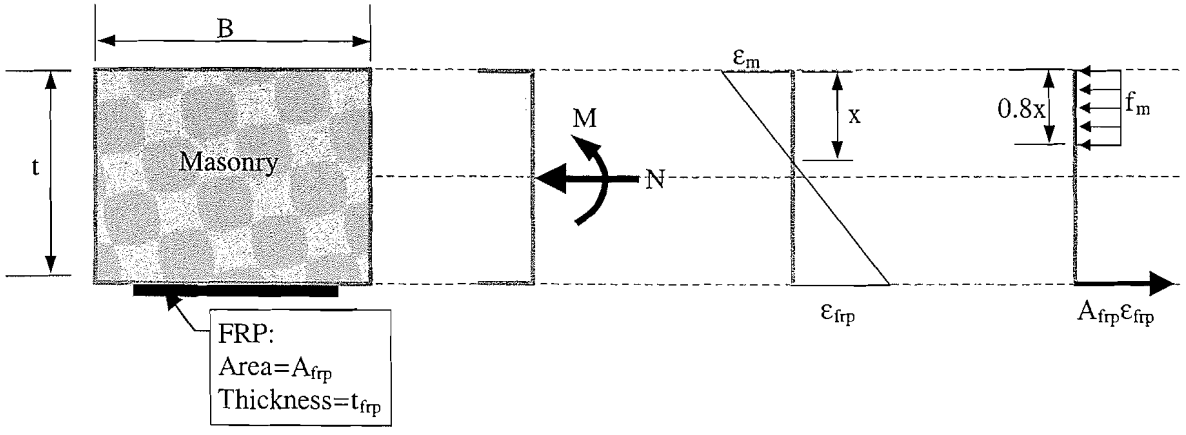

Figure 1. Ultimate state of an FRP strengthened rectangular masonry cross-section

Because the stress–strain relationship is linear until failure for most types of FRP composites, the stress distribution on the cross-section may be approximately represented by Figure 1d. Integrating the stresses on the cross-section gives the axial force N and the bending moment M:

$$N = 0.8Bxf_m - A_{frp}\varepsilon_{frp}E_{frp} \quad (2a)$$

$$M = 0.8Bxf_m\left(\frac{t}{2} - 0.4x\right) + A_{frp}E_{frp}\varepsilon_{frp}\frac{t}{2} \quad (2b)$$

where E_{frp} is the Young's modulus of the FRP composite and f_m is the ultimate compressive strength of the masonry.

The cross-section may fail due to either rupture of the FRP composite or compression failure of the masonry. Because FRP composites are brittle materials so the latter failure mode is preferred. These different failure modes are considered separately as follows.

2.2. Masonry Compression Failure

If the maximum strain in the masonry reaches its ultimate strain ε_{mu} whilst the strain in the FRP composite ε_{frp} is smaller than its ultimate (rupture) strain $\varepsilon_{frp,rup} = f_{frp}/E_{frp}$, the cross-section fails due to compression failure of the masonry. Here f_{frp} is the ultimate strength of the FRP composite. Substituting $\varepsilon_m = \varepsilon_{mu}$ into Eqn 1 gives the strain in the FRP composites at failure:

$$\varepsilon_{frp} = \left(\frac{t}{x} - 1\right)\varepsilon_{mu} \quad (3)$$

Substituting Eqn 3 into Eqns 2a and b gives

$$\frac{N}{f_mBt} = 0.8\frac{x}{t} - \frac{A_{frp}\varepsilon_{mu}E_{frp}}{f_mBt}\left(\frac{t}{x} - 1\right) \quad (4a)$$

$$\frac{M}{f_mBt^2} = 0.8\frac{x}{t}\left(\frac{1}{2} - 0.4\frac{x}{t}\right) + \frac{A_{frp}\varepsilon_{mu}E_{frp}}{f_mBt}\left(\frac{t}{x} - 1\right)\frac{1}{2} \quad (4b)$$

Let

$$\omega_{frp} = \frac{\varepsilon_{mu}E_fA_f}{f_mBt} \quad (5a)$$

$$\overline{M} = \frac{M}{f_mBt^2} \quad (5b)$$

$$\overline{N} = \frac{N}{f_mBt} \quad (5c)$$

being the normalised FRP fraction, bending moment and axial force respectively. Eqns 4a and b become

$$\overline{N} = 0.8\frac{x}{t} - \omega_{frp}\left(\frac{t}{x} - 1\right) \quad (6a)$$

$$\overline{M} = 0.4\frac{x}{t}\left(1 - 0.8\frac{x}{t}\right) + 0.5\omega_{frp}\left(\frac{t}{x} - 1\right) \quad (6b)$$

If the compressive force $\overline{N}$ is known, the height of the compressive area of the masonry x can be found from Eqn 6a:

$$\frac{x}{t} = \frac{1}{1.6}\left[\overline{N} - \omega_{frp} + \sqrt{(\omega_{frp} - \overline{N})^2 + 3.2\omega_{frp}}\right] \quad (7)$$

The M–N relationship can thus be determined from Eqns 6 and 7.

The above equations apply when the stress in the FRP is tensile, i.e. $x/t < 1$. When $x/t \geq 1$ (i.e. $\overline{N} \geq 0.8$), Eqns 6b and 7 may be replaced by ignoring the compressive strength of the FRP (setting $\omega_{frp} = 0$):

$$\overline{M} = 0.4\frac{x}{t}\left(1 - 0.8\frac{x}{t}\right) \quad (8a)$$

$$\frac{x}{t} = \frac{1}{0.8}\overline{N} \quad (8b)$$

Equation 8 also applies for all un-strengthened cross-sections, independent of the value of $\overline{N}$.

2.3. FRP Rupture Failure

If the FRP composite reaches its ultimate strength before the maximum strain in the masonry reaches its ultimate strain ε_{mu}, the cross-section fails due to rupture of the FRP. The strain in the FRP composite at failure is known in this case. Substituting $\varepsilon_{frp} = \varepsilon_{frp,rup}$ into Eqns 2a and b gives

$$\frac{x}{t} = \frac{1}{0.8}(\overline{N} + \omega_{frp}\xi) \quad (9a)$$

$$\overline{M} = 0.4\frac{x}{t}\left(1 - 0.8\frac{x}{t}\right) + 0.5\omega_{frp}\xi \quad (9b)$$

where ξ is the ultimate strain ratio of FRP to masonry

$$\xi = \frac{\varepsilon_{frp,rup}}{\varepsilon_{mu}} \tag{10}$$

2.4. Balanced Failure

The boundary between the masonry compression failure and the FRP rupture failure modes lies at when the FRP composite and the masonry both reach their ultimate strains simultaneously, i.e.

$$\varepsilon_m = \varepsilon_{mu} \quad \text{and} \quad \varepsilon_{frp} = \varepsilon_{frp,rup} \tag{11}$$

Substituting Eqn 11 into Eqns 2a and 3 gives the critical FRP fraction for this balanced failure mode:

$$\omega_{frp,cr} = \frac{0.8}{\xi + \xi^2} - \frac{\bar{N}}{\xi} \tag{12}$$

2.5. Numerical Results

When calculating the moment capacity for a given normalised axial force $\bar{N}$, the critical FRP fraction $\omega_{frp,cr}$ needs to be calculated using Eqn 12 first. If the actual FRP fraction is greater than $\omega_{frp,cr}$, the cross-section fails due to masonry compression failure and Eqns 6 and 7 should be used. Otherwise the cross-section fails due to FRP rupture and Eqn 9 should be used instead.

Figure 2 shows the critical FRP fraction for various FRP to masonry ultimate strain ratios. Clearly, more FRP composites are needed to prevent FRP rupture failure for small axial forces and small ultimate strain ratios of FRP to masonry. The ultimate strain ratio of FRP to masonry ξ has a very significant effect on the critical FRP fraction. If $\xi = 1$, the cross-section will always fail due to crushing of masonry when the normalised axial force $\bar{N}$ is greater than 0.4. If ξ increases to 3, FRP rupture will not occur when $\bar{N} > 0.2$. For commonly used FRP composites and masonry, ξ is usually greater than 3.

Figure 3 shows the effect of the FRP fraction ω on the normalised moment $\bar{M}$ for various axial forces. As ω increases from zero, $\bar{M}$ increases very fast initially but remains almost unchanged when ω becomes large. This indicates that it is most economical to strengthen the structure when only a small amount of FRP composite is needed. Further increase of the load bearing capacity by using more FRP composite is uneconomical. The figure also shows that the strengthening is most effective if the axial force is small.

Figure 4 shows the M–N relationship for various ω values, which again shows that the moment capacity can be most effectively increased when the compression force is small. This implies that this strengthening

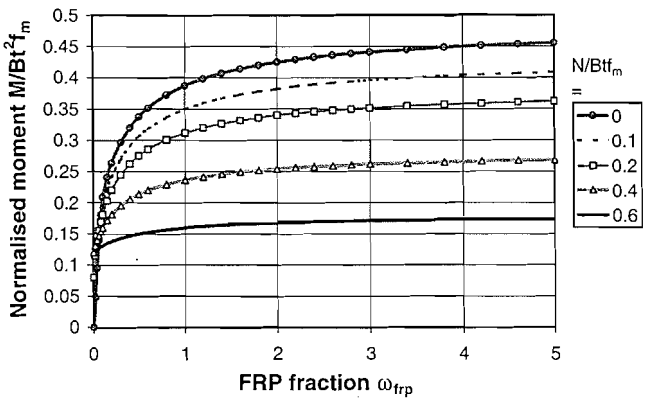

Figure 3. Normalised moment versus FRP fraction

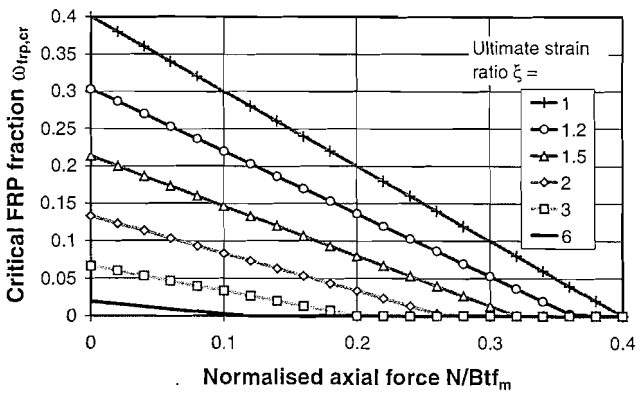

Figure 2. Minimum FRP fraction to prevent FRP rupture failure

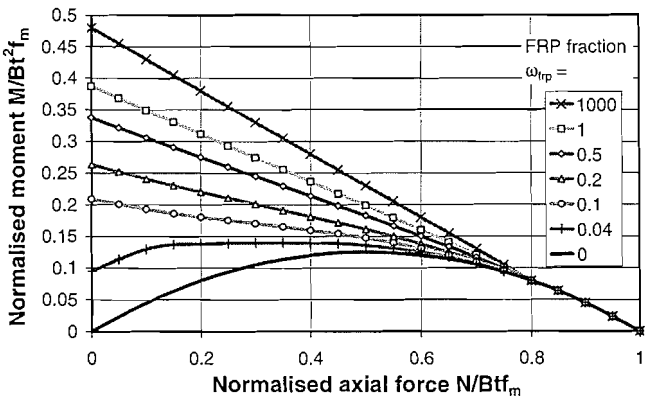

Figure 4. M–N relationship for various FRP fractions

technique may be most effectively used for shallow arch bridges.

It may be noted that a similar analysis for masonry structures strengthened using bonded FRPs was presented by Triantafillou (1998a). However, this was incomplete because no analysis for ω less than the critical value was presented. It also contains errors, even after a correction in Triantafillou (1998b) because he predicted that the moment capacity decreases as ω increases when the axial force exceeds certain values. The work here thus represents a fuller and more rigorous analysis.

3. A NEW MECHANISM ANALYSIS METHOD FOR STRENGTHENED MASONRY ARCH BRIDGES

3.1. Virtual Work Relationship

For a plastic hinge subjected to a virtual rotation θ (Figure 5), the virtual work done by the internal forces M and N is:

$$W = \left[M - N\left(\frac{t}{2} - x\right)\right]\theta \qquad (13)$$

For the load distribution and a failure mechanism of an arch bridge as shown in Fig. 6, the virtual work relationship may be expressed as

$$\int p\Delta_p \mathrm{d}x + \sum_{j=1}^{3} \Delta_j W_j + D_{\mathrm{hf}} H_{\mathrm{f}} = \sum_{i=A}^{D} \left[M_i - N_i\left(\frac{t}{2} - x_i\right)\right]\theta_i \qquad (14)$$

in which W_j is the dead weight for each of the blocks; H_f is the total horizontal forces provided by the passive resistance of the fill; the virtual displacements Δ_p at loading places, Δ_j at the gravity centre of the jth block and Δ_{Hf} at the centre of horizontal fill resistance force, and the virtual rotation θ_i of each hinge can be obtained from basic kinematics. Forces and displacements are downwards and rightwards positive here.

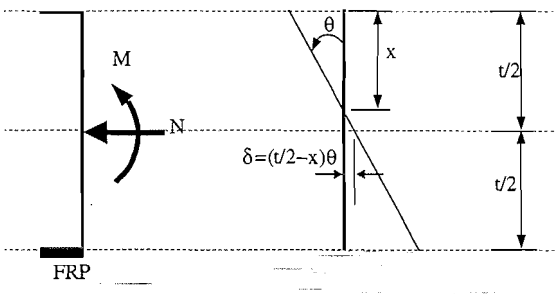

Figure 5. Virtual deformations at a hinge

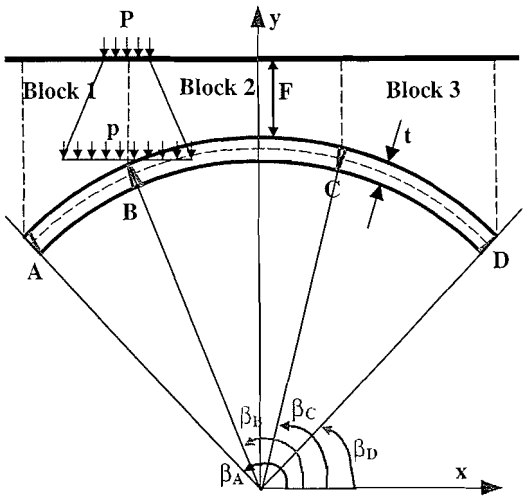

Figure 6. Load distribution and mechanism

The internal forces at each of the hinges M_i and N_i can be found from the equilibrium for the given mechanism, together with the appropriate M–N relationship, using an iterative procedure. Depending on whether the value of ω_{frp} is greater than $\omega_{\mathrm{frp,cr}}$, either Eqns 6 and 7 or 9 should be used as appropriate. If there is no FRP, or the bending moment is opposite to the direction as shown in Figure 5, Eqn 8 should be used. An unstrengthened masonry arch structure is thus a special case here.

The collapse load for a given mechanism can thus be determined by using the virtual work relationship (Eqn 14) and the static equilibrium. It may be noted that the eccentric compression force at a hinge can be outside the ring if the FRP is effective (i.e. in tension).

3.2. Determination of Minimum Collapse Load and Its Corresponding Hinge Positions

In traditional mechanism analysis, the arch ring is divided into a set of (typically 50) elements. The minimum collapse load $P_{\min}$ and its corresponding hinge positions have to be obtained by trial and error (Page 1993). This is a tedious process. A new method is thus devised here to obtain the minimum collapse load and its corresponding hinge positions.

In this new method, the arch ring is not divided into blocks, so that all the hinge positions can vary continuously within the ring. For simplicity, Hinge B is assumed to be located right beneath the centre of the loading here. However, there should be no difficulties in the following analysis to allow the position of Hinge B to vary by removing this assumption.

For the given four-hinge mechanism, the collapse load P can be found from the virtual work and static

equilibrium for each set of kinematically admissible hinge positions. As Hinge B is fixed as above, P is thus a function of the positions of Hinges A, C and D but the explicit expression of this function is unknown. Therefore, the problem is to find a set of kinematically admissible hinge positions so that the collapse load is minimised.

If the hinge positions are expressed in terms of angles β (can also be any other geometrical measures), the problem can be mathematically expressed as

$$\text{Minimise} \qquad P(\beta) \tag{15a}$$

where

$$\beta = \{\beta_A, \beta_C, \beta_D\}^T \tag{15b}$$

$$\text{Subject to} \qquad \beta_C > \beta_D \tag{15c}$$

$$\beta_{min} = \{\beta_{B0}, \beta_{D0}, \beta_{D0}\}^T \le \beta_{max} = \{\beta_{A0}, \beta_{B0}, \beta_{B0}\}^T \tag{15d}$$

$$\text{kinematically admissible} \tag{15e}$$

in which β_{A0}, β_{B0}, and β_{D0} are angle positions of the two springings and the load (Figure 6) and represent the limits to which Hinges A, C and D may vary (Eqn 15d). The constraint Eqn 15c is used here to keep the hinges in the right order. Constraint Eqns 15c and d together ensure that the solution will be in the order of $\beta_A > \beta_B > \beta_C > \beta_D$. The constraint Eqn 15e is used to ensure that the obtained mechanism is kinematically admissible. It needs to be quantified in numerical analysis and this was done here by using an indicator KA which equals 1 if a set of the hinge positions is kinematically admissible and −1 if inadmissible. The constraint Eqn 15e thus becomes

$$KA > 0 \tag{16}$$

This is a constrained nonlinear optimisation problem (or constrained nonlinear programming problem): to minimise the objective function P subject to constraints of Eqns 15c–e. Many constrained nonlinear programming methods are available. Detailed descriptions of nonlinear programming methods can be found in many textbooks (e.g. Himmelblau 1972, Avriel 1976). The Complex Method proposed by Box (1965) was used in this study. Detailed description of the Complex Method is beyond the scope of this paper. Interested readers may consult Box (1965) or textbooks in nonlinear programming (e.g. Himmelblau 1972, Avriel 1976).

A small computer program has been developed to carry out the analysis. The only inputs required are the material and geometrical properties. The program automatically reports the predicted minimum collapse load and the corresponding hinge positions. The effort required from a user of this program is thus minimal. Readers interested in this program may approach the author for more information.

4. NUMERICAL ANALYSIS OF AN EXAMPLE BRIDGE

4.1. The Unstrengthened Bridge

The Bolton full scale model segmental bridge tested by Melbourne and Walker (1989) was used here to apply the devised analysis method. Details of the bridge were obtained from Page (1993). The square span of the arch ring was 6 m and the total width was 6 m. A schematic drawing of the bridge geometry is shown in Figure 7. The ring was constructed using concrete bricks. The brickwork had a density of 21952 kN/m^3 and a compressive strength of 11.2 MPa. The fill was limestone with a density of 21364 kN/m^3 and internal friction angle $\phi = 54°$. The ultimate strain of the concrete brick was assumed to be 4000 $\mu\varepsilon$ in the analyses in the following two sections.

A 'line' load with 750 mm width was applied. The bridge failed with a 4 hinge mechanism and the maximum measured load was 1170 kN. The prediction of the above analysis method was 1144 kN, representing an error of less than 2.5%. However, the error of prediction is expected to be much bigger than this for deeper bridges because of the inherited limitation of mechanism analysis.

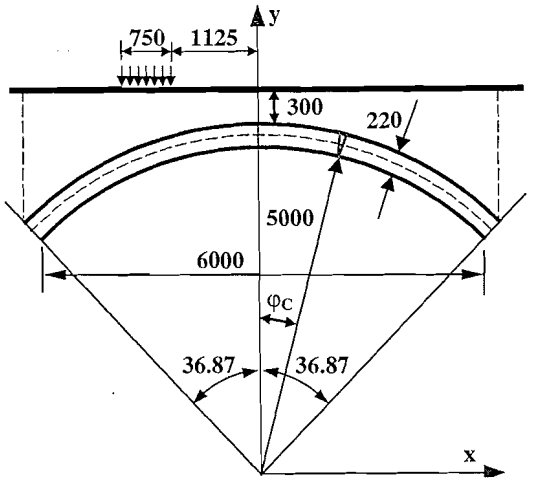

Figure 7. Geometry of the Bolton full scale model bridge (Melbourne and Walker 1989)

4.2. Effect of Strengthening on Collapse Load

The above bridge is now assumed to be strengthened by bonding an FRP sheet on the intrados. It is assumed that a carbon fibre reinforced polymer (CFRP) composite with strength f_{frp} = 2400 MPa and Young's modulus $E_{frp} = 2 \times 10^5$ MPa is used. Two options are considered:

a) The FRP is bonded on the full intrados, but not anchored in the abutments (i.e. not effective for Hinge D). Because both the loading position and the position of Hinge B were fixed in this analysis, the effect will be minimal whether the full intrados is strengthened given that Hinge B is always strengthened. The only effect which may arise is that when the predicted position of Hinge D is not at the springing. However, the intrados should be fully strengthened in practice because of moving loads.
b) The FRP is bonded on the full intrados and fully anchored in the abutments so that it is effective for Hinge D as well.

Figures 8 and 9 show that the collapse load can be very significantly increased even by bonding a very thin sheet. If a 0.1 mm thick CFRP sheet is used, the predicted collapse load increases from 1144 kN for the unstrengthened bridge, to 1906 kN (67% increase) if only Hinge B is strengthened and 2181 kN (91% increase) if both Hinges B and D are strengthened. By bonding a 1 mm thick FRP, the collapse load is further increased to 2932 kN (156% increase) and 3424 kN (199% increase) for the two strengthening schemes respectively. However, it is clear that it is most effective to use very thin (e.g. 0.1 mm) sheets in this case.

It may also be noted that the current theoretical predictions are the same for bonding a 0.1 mm sheet in the full intrados, and for bonding 1 mm × 50 mm strips @ 500 mm centres. The latter is indeed more convenient to apply in practice. However, the former is the preferred choice for two reasons. Firstly, the continuous sheet can provide transverse strengthening/constraint so that longitudinal cracks may be prevented from developing. Secondly, the analysis has so far assumed that there is a perfect bond between the masonry and the FRP. However, this is unlikely to be true especially for deep arches. A recent study on the bond behaviour between FRP composites and concrete (Chen and Teng 2000, 2001) shows that the use of thin sheets is much more effective than thick sheets. The Young's modulus has also a very significant effect in this respect. More details can be found in Chen and Teng (2001) and Teng et al. (2001).

Figures 8 and 9 demonstrate clearly that it is a very effective measure to anchor the FRP in the abutments, so this should be adopted wherever possible.

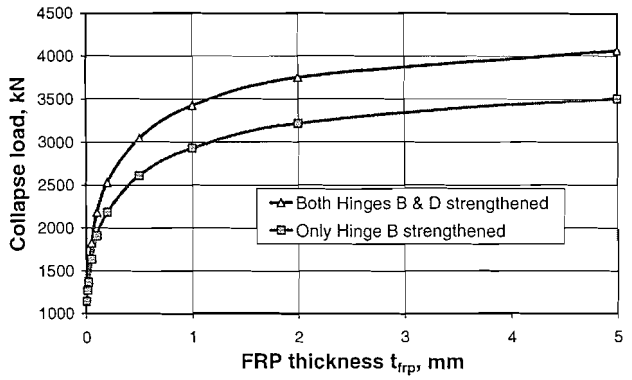

Figure 8. Effect of FRP thickness on the collapse load

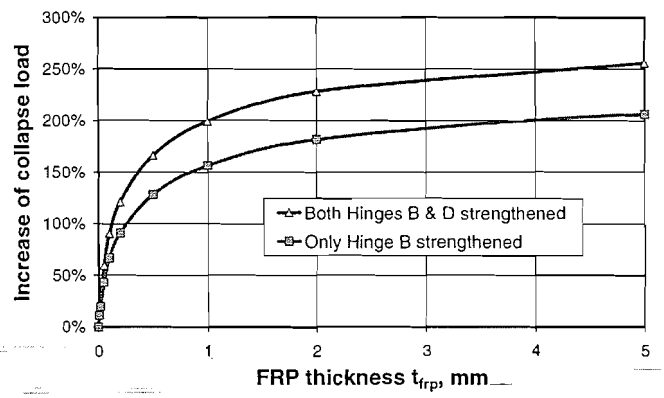

Figure 9. Increase of collapse load

4.3. Effect of Strengthening on Hinge Positions

The predicted positions for Hinges A and D are always at the springings in this example. This may be due to the fact that this is a very shallow arch.

The predicted position for Hinge C varies as the thickness of the FRP sheet changes. Figure 10 shows this position measured by using the angle from vertical (φ_C in Figure 7). If only Hinge B is strengthened, the

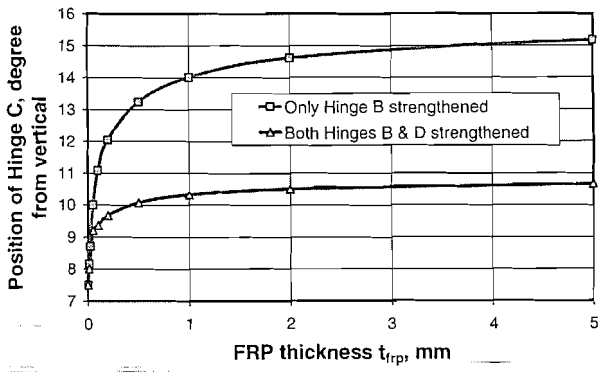

Figure 10. Effect of FRP thickness on hinge position

angle increases from 7.5° (on the ring central 0.67 m from the symmetry) for the unstrengthened bridge, to 11.1° (0.98 m from the symmetry) when t_{frp} = 0.1 mm and close to the three quarters for t_{frp} = 5 mm. A similar trend is seen, but the position change is much smaller if both Hinges B and D are strengthened.

If the ring is divided into 50 blocks as in traditional mechanism analysis, each block represents 1.5° which will make it impossible to produce smooth curves as shown in Figure 10. This further demonstrates the advantage of the new method devised in this study.

5. CONCLUSIONS

This paper has presented an initial study on strengthening masonry arch bridges using externally bonded FRPs on the intrados. The *M–N* relationship for a rectangular masonry cross section strengthened with FRP has been developed and it has been used in the mechanism analysis of strengthened bridges. A new mechanism analysis method has been developed. It finds the minimum collapse load, and its corresponding hinge positions, by using a constraint optimisation method. The arch ring is not needed to be divided into artificial blocks so that the hinge positions can change continuously. The analysis procedure is fully automatic and is of high efficiency because it needs minimal user input. Initial numerical results have shown that it is very effective to strengthen masonry arch bridges by bonding a thin FRP sheet on their intrados. The strengthening effect can be significantly enhanced by anchoring the FRP in the abutments.

REFERENCES

Avriel, M. (1976). *Nonlinear Programming: Analysis and Methods*, Prentice-Hall, Inc., New Jersey.

Box, M.J. (1965) "A new method for constraint optimisation and a comparison with other methods", *Computer Journal*, Vol. 8, pp. 42–52.

Chen, J.F. and Teng, J.G. (2000) "A new bond strength model for FRP and steel plates attached to Concrete", *Proceedings of the 6th International Conference on Structural Failure, Durability and Retrofitting*, 14–15 September Singapore, pp. 229–136.

Chen, J.F. and Teng, J.G. (2001) "Anchorage strength models for FRP and steel plates bonded to concrete", *Journal of Structural Engineering*, ASCE, Vol. 127, No. 7, pp. 784–791.

Department of Transport (1993) "The assessment of highway bridges and structures", Part 3, BD 21/93; Part 4, BA 16/93.

Himmelblau, D.M. (1972). *Applied Nonlinear Programming*, McGraw-Hill, Inc., New York.

Hughes, T.G. (1995) "Analysis and assessment of twin-span masonry arch bridges", *Proceedings of the Institution of Civil Engineers: Structures and Buildings*, Vol. 110, pp. 373–382.

Hughes, T.G. and Blackler, M.J. (1997) "A review of the UK masonry arch assessment methods", *Proceedings of the Institution of Civil Engineers: Structures and Buildings*, Vol. 122, pp. 305–315.

Hughes, T.G., Davies, M.C.R. and Taunton, P.R. (1998) "Small scale modelling of brickwork arch bridges using a centrifuge", *Proceedings of the Institution of Civil Engineers: Structures and Buildings*, Vol. 128, pp. 49–58.

Melbourne, C. and Walker, P.J. (1989) "Load test to collapse on a full scale model six meter span brick arch bridge", *Department of Transport*, TRRL contractor Report 189, Transport Research Laboratory, Crowthorne.

Melbourne, C., Gilbert, M. and Wagstaff, M. (1997) "The collapse behaviour of multispan brickwork arch bridges", *The Structural Engineer*, Vol. 75, No. 17, pp. 297–305.

Page, J. (1993) *Masonry arch bridges: state of the art reviews*, HMSO publications.

Peaston, C. and Choo, B.S. (1996) "Predicting the capacity of sprayed concrete strengthened masonry arch bridges: A comparison experimental and analytical data", *ICCI'96, Fibre Composites in Infrastructure (ed by H. Saadatmanesh & M.R. Ehsani), Proceedings of the First International Conference on Composites in Infrastructure*, Arizona, USA, pp. 91–95.

Ponniah, D.A. and Prentice, D.J. (1998) "Load-carrying capacity of masonry arch bridges estimated from multi-span model tests", *Proceedings of the Institution of Civil Engineers: Structures and Buildings*, Vol. 128, pp. 81–90.

Prentice, D.J. (1996) "An appraisal of the geotechnical aspects of multi-span masonry arch bridges", PhD thesis, Edinburgh University.

Teng, J.G., Chen, J.F., Smith, S.T. and Lam, L. (2002) *FRP-Strengthened RC Structures*, John Wiley and Sons, Chichester, U.K.

Triantafillou, T.C. (1998a) "Strengthening of masonry structures using epoxy-bonded FRP laminates", *Journal of Composites for Construction*, ASCE, Vol. 2, No. 2, pp. 96–104.

Triantafillou, T.C. (1998b) "Errata", *ASCE Journal of Composites for Construction*, Vol. 2, No. 4, p. 203.

Dr Jian-Fei Chen is a Lecturer in structural engineering in the School of the Built Environment, the University of Nottingham, UK. He received his BSc and MSc from Zhejiang University in China and PhD from Edinburgh University. He has interest in many areas in civil engineering, including reinforced concrete, masonry and steel structures; space and shell structures; granular solids flow and wall pressures in silos and inverse problems.